

THERMODYNAMIC, KINEMATIC, AND RADAR PARAMETERS OF ISOLATED
TORNADOES WITH AND WITHOUT NWS WARNING

A Thesis
presented to
the Faculty of the Graduate School
at the University of Missouri-Columbia

In Partial Fulfillment
of the Requirements for the Degree
Master of Science

by
PATRICIA VAN BUREN
Dr. Neil I. Fox, Thesis Supervisor
MAY 2017

The undersigned, appointed by the dean of the Graduate School, have examined the thesis entitled

THERMODYNAMIC, KINEMATIC AND RADAR PARAMETERS OF ISOLATED
TORNADOES WITH AND WITHOUT NWS WARNING

presented by Patricia F. Van Buren,
a candidate for the degree of master of science,
and hereby certify that, in their opinion, it is worthy of acceptance.

Associate Professor Neil Fox

Professor Patrick Market

Associate Professor Sonja Wilhelm Stanis

ACKNOWLEDGEMENTS

First and foremost, I would like to thank my mother, Ruth DeVay, and father, Peter Van Buren, for the constant love and support as I moved away from home and dove into the stress-filled life of a Master's student. I would like to thank my advisor, Dr. Neil Fox, for his time and effort, dealing with me every day, and continuously pushing me. Thank you to the rest of my committee, Dr. Patrick Market and Professor Sonja Wilhelm Stanis, for your time and patience as I struggled toward the end. And a special thanks to Dr. Patrick Market for listening (maybe half listening?) to me complain, letting me cry in his office, and reminding me I can do anything I set my mind to when the stress of Graduate School made me question my abilities.

Thank you to my friends back home for all of your support and encouragement. Thank you to my fellow graduate colleagues for keeping me in line, reminding me of due dates/how to graduate, and always being ready to grab some drinks. Thank you Chelsy Simpson for always feeding me and making sure I'm alive, and thank you Micheal Simpson for the endless amount of coding and MatLab help; I could not have finished this without either of you.

TABLE OF CONTENTS

ACKNOWLEDGEMENTS	ii
LIST OF FIGURES	iv
LIST OF TABLES	v
ABSTRACT.....	vi
CHAPTER 1: INTRODUCTION.....	1
1.1 Statement of Thesis.....	1
CHAPTER 2: LITERATURE REVIEW	4
2.1 Radar History.....	4
2.2 Brotzge and Erickson (2009 and 2010).....	7
2.3 Smith et al. (2012) and Thompson et al. (2012).....	13
2.4 Tornado Probability of Detection and Lead Time using Convective Mode and Environmental Parameters.....	15
2.5 Warning Decision Support System – Integrated Information.....	16
2.6 Preliminary Study.....	19
CHAPTER 3: METHODOLOGY	20
3.1 Data Sorting.....	20
3.2 WDSS and MatLab.....	24
CHAPTER 4: RESULTS AND DISCUSSIONS	32
4.1 Thermodynamic and Kinematic Parameters at Time of Event.....	32
4.2 Radar Parameters – Warned vs. Unwarned.....	35
4.3 Radar Parameters – WARN vs. Nontornadic Cells.....	38
4.4 Radar Parameters – NOWARN vs. Nontornadic Cells.....	44
CHAPTER 5: CONCLUSIONS	47
5.1 Conclusion.....	47
5.2 Future Work.....	48
APPENDIX.....	50
REFERENCES.....	61

List of Figures

Figure 3.1 <i>CellVort</i> imagery result for event 20130831 prior to tornado formation. The yellow cell is the tornadic cell (assigned reference number 6). This event did receive a NWS warning.....	27
Figure 3.2 Time of tornado (WARN) <i>CellVort</i> imagery result for event 20130831. The dark red cell is the tornadic cell (assigned reference number 10).....	28
Figure 3.3 <i>CellVort</i> imagery result for event 20130730 prior to tornado formation. The yellow cell is the tornadic cell (assigned reference number 5). This event did not receive a NWS warning.....	28
Figure 3.4 <i>CellVort</i> imagery result for event 20130730 (NOWARN) at time of tornado formation. The red cell is the tornadic cell (now assigned reference number 8).....	29
Figure 4.1 Box and whisker plots of azimuthal shear (s^{-1}) at time before tornado (NOWARN), time before (WARN), time of warning (NTC), and time of warning (WARN).....	40
Figure 4.2 Box and whisker plots of maximum divergence (s^{-1}) among all time steps and events analyzed. From left to right: NOWARN at time of tornado formation, WARN at time of tornado formation, NTCs at time of tornado formation, WARN before formation, NOWARN before formation, NTC at time of warning, and WARN at time of warning.....	41
Figure 4.3 Box and whisker plots of minimum divergence (s^{-1}) (convergence) among all time steps and events analyzed. From left to right: NOWARN at time of tornado formation, WARN at time of tornado formation, NTCs at time of tornado formation, WARN before formation, NOWARN before formation, NTC at time of warning, and WARN at time of warning.....	41
Figure 4.4 Box and whisker plots of azimuthal shear (s^{-1}) at time of tornado for NOWARN, NTC and WARN events.....	46

List of Tables

Table 3.1 Excel workbook of isolated tornadoes after completed data sorting. From left to right: date, time, Weather Forecasting Office (WFO), whether or not a warning was issued (Y = Yes, N = No), F-scale magnitude, state, distance tornado occurred from the WFO, latitude, and longitude. These events and their associated parameters were found by utilizing RUC-II analysis soundings.....	22
Table 3.2 Excel workbook of isolated tornado events within 150km range of radar, sorted by date.....	26
Table 4.1 P-values and means for thermodynamic and kinematic parameters at time of tornado between WARN and NOWARN. Parameters highlighted are those that are statistically significant at 95% confidence interval.....	33
Table 4.2 Resulting p-values from the Student's t-test comparison of before tornado formation between WARN and NOWARN. No results were significant at 95% confidence interval.....	36
Table 4.3 Resulting p-values from the Student's t-test comparison at Time of Tornado between WARN and NOWARN as well as their associated means. Results statistically significant at a 95% confidence interval are highlighted.....	37
Table 4.4 Resulting p-values from the Student's t-test comparison of tornadic cell and nearby nontornadic cells at time of warning as well as the means. Results statistically significant at a 95% confidence interval are highlighted.....	39
Table 4.5 Resulting p-values from the Student's t-test between tornadic cell and nearby nontornadic cells at time of tornado and their associated means. The one parameter statistically significant at a 95% confidence interval is highlighted.....	43
Table 4.6 Resulting p-values from the Student's t-test comparing tornadic cells with no warning and nontornadic cells that occurred nearby the tornadoes with warnings, as well as their associated means. Results statistically significant at a 95% confidence interval are highlighted.....	45

Thermodynamic, Kinematic, and RADAR Parameters of Isolated Tornadoes

With and Without NWS Warning

Patricia Van Buren

Dr. Neil Fox, Thesis Supervisor

Abstract

Tornadoes are a rapidly forming weather phenomenon that forecasters may have difficulty anticipating. A tornado warning is issued when atmospheric conditions are imminent for formation or a tornado has already formed and been confirmed. The purpose of this research was to find what, if any, atmospheric parameters and radar variables that may differ between isolated tornadoes that were anticipated by an official NWS Tornado Warning (WARN) versus isolated tornadoes that occur without NWS warning (NOWARN). The hypothesis was that there is a distinct difference in wind shear and azimuthal shear between WARN and NOWARN events. A dataset of tornado events from 2004 – 2015 was obtained from previous work completed by Thompson et al. (2012) and Smith et al. (2012). The dataset was condensed to only isolated events by analyzing dates and times with NOAA's Interactive Radar Map Tool. Specifically, outbreaks and tornadoes embedded in a synoptic system were removed from the dataset. The data were further reduced to include years 2013 – 2015, months April – September, and geographic region between the Rocky and Appalachian mountain regions. Each event was then analyzed using the Iowa Environmental Mesonet Search for NWS Watch/Warning/Advisories Products by County/Zone or by Point (latitude and longitude). This left 57 isolated tornadoes that were not warned for and 39 that were. These events were analyzed using a paired Student's t-test among the thermodynamic and kinematic parameters given in the dataset. Radar analysis was done using MatLab and a code that picked out individual cells using a dBZ threshold of 35. The tornadic cell was analyzed among multiple radar parameters using paired Student t-tests to find any significant difference between WARN and NOWARN at time of tornado formation and 30 minutes before formation, as well as between nearby nontornadic cells. The results revealed shear, divergence and convergence as significantly different between the events. Although azimuthal shear resulted as statistically significant, it does not perform well when deciphering between tornadic and nontornadic cells. However, convergence and divergence appear to be an indicator of tornadic cells.

CHAPTER 1: INTRODUCTION

1.1 Statement of Thesis

Forecasting in the early days of the Severe Local Storms Center of the U.S. Weather Bureau in the 1950's was limited largely to pattern recognition, sounding analysis, and subjectively predicting changes in the convective environment. Advances in numerical modeling and detailed field observations have resulted in a greater physical understanding of the processes supportive of severe thunderstorms and tornadoes (Grams et al. 2011). According to Brotzge and Donner (2013), in 1986 tornado warning lead time was approximately five minutes with only 25% of tornadoes warned; by 2004, mean lead time was 13 minutes with about 75% of tornadoes warned. Operational meteorologists have benefited from a dramatic increase in the quantity and quality of numerical weather prediction model guidance since the mid-1990s with the advent of gridded model output and numerous sounding-derived parameters related to severe storm occurrence (Grams et al. 2011). Some forecasters tend to focus on synoptic scale motions, such as short-wave troughs and midlevel height falls, to forecast tornado events. However, as a storm enters its tornadic phase, significant smaller scale features evolve which numerical models have been unable to resolve (Klemp and Rotunno 1983).

The watch/warning system is typically most effective for strong tornadic systems because precursor atmospheric signals are often most evident in these cases. Watches serve to reinforce forecast areas already identified in severe weather outlooks and are used to alert the public to the developing conditions that might spawn a high impact event. Thus, most warnings are a natural outcome of the information that has preceded them, and ideally the public is ready to respond appropriately and effectively to the

hazard (Stensrud et al. 2009). Tornado warnings are issued by the National Weather Service when the radar reveals a signature implying tornado formation (i.e. hook echo, couplets, mesoscale detection), a tornado is seen by spotters, or otherwise deemed imminent by the forecaster. Despite the difficulty of each decision, the warning forecaster strives to warn on every tornado, with as much lead time as possible, while minimizing the number of false alarm warnings (Brotzge and Donner 2013). Insight to small-scale features is important for recognizing tornado development and accurate forecasting. Nevertheless, in lieu of these advances, a significant number of tornado warnings still are issued either simultaneously as the tornado forms or minutes after initial tornado formation but prior to tornado dissipation (Brotzge and Erickson 2009).

False alarms have been thought to give the public a sense of false dependability with weather forecasters if their forecast is inaccurate. Too many false alarms may lead to the public denying a severe weather forecast and therefore not following proper safety procedures. To refrain from issuing too many tornado false alarms, some forecasters may adopt a general policy of waiting to issue a tornado warning until after storm spotters have confirmed a tornado visually. For others, their warning confidence for a given situation simply may be too low to issue a warning until after a tornado has been confirmed (Brotzge and Erickson 2010). The fear of issuing a false alarm or lack of confidence of the forecaster leads to numerous warnings being issued after a tornado has already developed. The research of Brotzge and Erickson (2010) concluded that the ability to physically observe a tornado plays an essential role in the warning operations process. Tornadoes warned in succession are more likely to be warnings on tornadoes already in progress, whereas the first tornado warning of the day is likely a warning based

on the anticipation of what will occur (Brotzge and Erickson 2009). This leads to the impression that once the forecaster recognizes an outbreak, the probability of detection of those tornadoes within the outbreak increases. Brotzge and Erickson (2009) also noted that isolated, single tornado per day events have 10 times the ratio of zero and negative lead-time warnings than do days with 20 or more tornadoes. The fewer numbers of reported tornadoes per day, the greater chance that those tornadoes were not warned. For solitary tornado events, over half of all tornadoes were not warned (Brotzge and Erickson 2010). This implies that there may be something about the pre-tornadic environment of an isolated event that forecasters are not noticing until the tornado has already formed.

The purpose of this study is to understand what, if any, atmospheric parameters and RADAR variables are different between isolated tornadoes that are anticipated by NWS tornado warning and ones that are not warned. The hypothesis is that wind shear and azimuthal shear show statistically significant differences between isolated tornado events anticipated by a NWS warning (WARN) and isolated tornado events not anticipated by a NWS warning (NO WARN). More specifically, the authors believe the unwarned tornadoes do not possess a noticeable value of shear and therefore do not represent a well-known tornadic precursor on RADAR imagery.

CHAPTER 2: LITERATURE REVIEW

2.1 Radar History

The first radar was used not for weather forecasting, but instead to detect attackers from the air or sea. The use of radar to observe weather developed as an outcome of the intensive work on radar technology during World War II (Whiton et al. 1998). In 1935, a Scottish physicist and meteorologist, Sir Robert A. Watson-Watt, began investigating the use of electromagnetic waves to locate aircraft. In 1940, a radar of 10-cm wavelength was operated at the General Electric Corporation Research Laboratory in England where it is likely that the first weather echo was seen (Whiton et al. 1998). Research conducted at the Massachusetts Institute of Technology Radiation Laboratory showed that weather could be detected on certain types of radars out to ranges of 150 miles at 3- and 10-cm wavelengths (Whiton et al. 1998). Increased availability to electronics in the 1960s made it practical to create storm avoidance radar for aircrafts. By 1969, a few television stations in the Midwest U.S. had installed radars for the weather segments of their broadcasts. By the late 1980s, the Department of Commerce, Department of Defense, and Department of Transportation jointly fielded two highly sophisticated, ground-based Doppler weather radar systems, the Next-Generation Weather Radar (NEXRAD), now called the WSR-88D, and the DOT's Terminal Doppler Weather Radar (Whiton et al. 1998).

In 1988, the U.S. Congress authorized the modernization and restructuring of the NWS to benefit from the use of modern observational systems, as well as increasing the amount of professional meteorologists on staff (Serafin and Wilson 2000). Today, the

NWS operates 122 weather forecast offices (WFO) for both operational forecasting and research. Each WFO is responsible to produce forecasts and issue any warnings for their county warning area, whether it be marine, hydrological, fire, or meteorological. Each WFO is also responsible for aviation forecasts for nearby airports. Forecasts are produced by human interpretation of radar, satellite, and numerical models.

The WSR-88D has led to significant improvement in the short-range forecasts and warnings of severe thunderstorms, tornadoes, and flash floods (Serafin and Wilson 2000). The first possible tornado report in the United States occurred in July 1643 in Massachusetts, and, after nearly 300 years of these observations, U.S. Army Signal Corps Sergeant John P. Finley was placed in charge of investigating tornadoes and developing a forecast method (NOAA). Finley published 15 rules to identify likely tornado formation in 1888. NOAA's "Celebrating 200 Years" online magazine (http://celebrating200years.noaa.gov/magazine/tornado_forecasting/finley_rules.html) lists these 15 rules: 1) Presence of a well-defined low pressure area, 2) Slow progression of the low increasing flow northward of heat and moisture into the southeast quadrant, 3) A north-south or northeast-southwest orientation of a trough-like low, 4) The descent of a well-marked anticyclone in the rear of the low, 5) High temperature gradients, 6) Increasing wind velocities of the southeast, southwest, and northwest quadrants of the low, 7) Northward curve of the isotherms in the southeast quadrant and eastern portion of the southwest quadrant of the low, 8) Southward curve of the isotherms in the northwest quadrant and the northern portion of the southwest quadrant, 9) High temperature gradient between the noses of opposing curves of temperature, 10) Increasing high humidity in the southeast quadrant of the low, 11) Maximum areas of tornado frequency

for each state, 12) Occurrence of tornadoes in certain parts of the country, in certain months of the year, 13) Tornadoes frequently occur in groups with parallel paths, within a few miles of each other, 14) Tornadoes always occur in the southeast quadrant of a low several miles southeast of its center, 15) Easterly curve in the southwest and northwest quadrants of a line separating the northerly and southerly surface winds of the low (NOAA).

Continued research and technological advancements have significantly improved severe weather and tornado forecasting. Although pattern recognition is still a large part of forecasting, forecasters now have real-time information and model output at their fingertips. Today, severe weather forecasters use a combination of Doppler radar, enhanced satellite imagery, and sophisticated analysis programs to rapidly make essential life-saving decisions. Forecasters and researchers have at their disposal, in fractions of a second, a varying array of data that were once hand-plotted just 40 years ago (NOAA).

Radar imagery provides real-time precipitation estimates and azimuthal velocity, important for tornado forecasting. Weather radar is the primary tool used by warning forecasters to identify areas of potential tornado development. Radar reflectivity provides forecasters with a clear view of tornadic features and Doppler radial velocity shows horizontal wind shear, which is sometimes an early indication of tornado formation (Brotzge and Donner 2013). For enhanced tornado detection, automated detection algorithms, such as the WSR-88D mesocyclone and tornado detection algorithms, automatically identify radar-based tornado features and are displayed in real time within the Advanced Weather Interactive Processing System (AWIPS) (Brotzge and Donner 2013). A NWS forecaster will issue a tornado warning when formation is considered

likely or if one has already formed. This official warning is used to alert the public of the potential threat. The NWS vision for 2025 is to provide tornado warning lead times of 45 minutes or greater. If we are to continue to improve tornado warning lead times, special attention should be given to two specific areas: (i) warning on the first tornado of the day and (ii) warning on nontypical (weak and/or isolated) severe storms (Brotzge and Erickson 2009).

2.2 Brotzge and Erickson (2009 and 2010)

Brotzge and Erickson (2009) researched NWS tornado warnings with zero or negative lead times in an effort to better understand the causes for the delay. Zero lead-times mean a warning was issued simultaneously as the tornado formed; negative lead-times mean the warning was issued after the tornado formation but prior to tornado dissipation. The data used were a 5 year compilation of tornado warning reports from 2000 to 2004 obtained from NOAA/NWS. The database included 4604 positive lead-time events, 211 zero lead-time events, and 355 negative lead-time events (Brotzge and Erickson 2009). Zero lead-time events and negative lead-times were combined ($n=566$) to be collectively referred to as negative lead-times. The data were used to determine any significant difference among F-scale, geographical distribution, WFO, diurnal climatology, seasonal climatology, storm morphology, population density, distance from radar, and high-impact events (more than one tornado per event).

Brotzge and Erickson (2009) discuss four critical challenges faced by operational forecasters based on four outliers from their dataset. The first outlier event formed within a squall line, near dusk, approximately 170 km from the nearest radar. The second was

spawned by Hurricane Frances in 2004. The third formed from an undefined convective complex, approximately 205 km from the nearest radar, in a county with extremely low population density. The last outlier event formed after dark in another undefined convective complex. The four critical challenges demonstrated by these events are no parent classical supercell, lack of spotter reports, too far from the radar, and providing advance warning for situations in which many warnings are needed for a variety of severe weather conditions, such as Hurricane Frances (Brotzge and Erickson 2009).

The negative and zero lead-time events were first compared against F-scale ratings. Between 2000 and 2004, only 12 of the 566 zero or negative lead-time tornado events that occurred were classified as F3 or higher (Brotzge and Erickson 2009). This poses the question; what other factors are affecting this? Are the tornadoes not warned for in advance because they are too far from the radar or because they occurred in the middle of a field with no storm spotter reports? According to Brotzge and Erickson (2009), no statistical relationship was found between negative lead times and distance from the radar, and no statistical significance was found relating negative lead time and county population density.

To test the significance of geographic location, tornado warnings were sorted into four broad geographic regions: southeast, midwest/east, plains, and west (Brotzge and Erickson 2009). For both positive and negative lead-times, the plains region was found to be significantly different from each of the other three regions (Brotzge and Erickson 2009). More positive lead-times and less negative lead-times occur in the plains. It was concluded may be due to the prevalent tornado activity in the plains, giving the forecasters in that area more experience with the warning process. Next, Brotzge and

Erickson (2009) compared events based on WFO. All WFOs with over 100 tornado warnings during the 5-yr study period averaged less than 10% of warnings with negative lead-time, meaning WFOs that experience more tornadic activity have a better chance of warning for the event prior to formation. This also demonstrates that WFO warning operations can significantly impact warning results (Brotzge and Erickson 2009).

In regards to seasonal climatology, Brotzge and Erickson (2009) found that nationwide, tornadoes with zero or negative lead times peaked during July and August with a relative minimum in May. To further analyze this, Brotzge and Erickson (2009) sorted and plotted seasonal climatology impact based on geographic region. They found that tornadoes with zero and negative lead-time warnings peaked in the southeast and west regions in July and August, the peak in the Midwest was observed in July, and in the plains region the peak was in September. In regards to storm morphology, little noticeable difference was found in storm type between those tornado warnings with positive lead time and tornadoes with zero or negative lead time.

One trend was found with diurnal climatology impact; above-average numbers of zero and negative lead-time warnings are used between 1300 and 1800 local time. This trend likely captures the difficulty in warning on the first tornado of the day (Brotzge and Erickson 2009) and is extremely relevant to this current research of isolated tornadoes. If the first tornado of the day is proven to be the most difficult and less likely to warn for, then, ideally, isolated tornadoes should have very few positive lead-time warnings.

Brotzge and Erickson (2009) extended their research to high-impact events to test the hypothesis that the first tornado of the day is more difficult to warn in advance. Their

results revealed that the more warned tornadoes per day, the smaller the ratio of zero or negative lead-time warnings. The average tornado warning lead-time increased from 11.8 minutes with a single tornado warning per day to 16+ minutes for tornadoes on days with four or more confirmed warnings (Brotzge and Erickson 2009). It was also pointed out that forecasters may be reluctant to issue the first warning of the day in order to minimize false alarms.

The main takeaway from Brotzge and Erickson (2009) pertaining to this current research is: *In general, the more isolated the tornado event, the less is the likelihood that an advance warning is provided.* Isolated single tornado per day events have 10 times the ratio of zero and negative lead-time warnings than do days with 20 or more tornadoes (Brotzge and Erickson 2009).

Brotzge and Erickson (2010) expanded upon their previous research, but this time with a focus on tornadoes without NWS warning. Tornado data were collected from the same 5 years (2000 to 2004) and were sorted/evaluated the same. The first hypothesis tested by the authors was that larger and violent tornadoes are more likely to be warned and recognized from radar. When the dataset was sorted by F scale and whether or not a warning was issued, the results indicated the stronger the tornado rating, the greater the chance that tornado was warned (Brotzge and Erickson 2010). Tornadoes with no NWS warning were also analyzed for significance among geographical distribution, diurnal climatology, seasonal climatology, storm morphology, population density, distance from radar, and high-impact events (more than one tornado per event).

The plains region had a significantly lower ratio of unwarned tornadoes, just over 20% when compared to other regions, whereas the west has over double the ratio of unwarned tornadoes at 42% (Brotzge and Erickson 2010). Since tornadic activity is more prevalent in the plains, it is easy to see how forecasters in that area may have more experience recognizing the precursor environment in order to issue a successful warning. To test if this is the case, the tornado data were sorted by WFO area in which each tornado occurred. Results showed that WFOs with a small number of documented tornadoes during the 5 year period have a relatively high percentage of unwarned tornadoes, and WFOs with a high number of tornadoes generally warn on at least of 70% of the tornadoes reported within their county warning area (Brotzge and Erickson 2010).

Diurnal climatology revealed that, in general, tornadoes that occurred at night, during the morning, and during the early afternoon hours sustained a much higher unwarned ratio than during the late afternoon hours (Brotzge and Erickson 2010). Seasonal climatology results were similar to the results of Brotzge and Erickson 2009. Those months with the greatest numbers of tornado reports have the lowest ratios of unwarned tornadoes (i.e. July and August), while those months with relatively few tornado reports (i.e. January) have the highest ratios of unwarned tornadoes (Brotzge and Erickson 2010).

When storm classification was evaluated, Brotzge and Erickson (2010) found that many of the unwarned cases were more difficult to classify than those storms with warning lead time. These storms appeared to be evolving as tornado formation occurred. Brotzge and Erickson (2010) also found that the mean pathlength of a warned tornado was 4.1 km compared to a pathlength of 2.4 km of an unwarned tornado. It was also

found that the greater the county population density, the smaller the percentage of recorded tornadoes that were warned. The ratio of weak (F0 and F1) tornadoes not warned increases with increasing population density. These results may reflect the possibility that weak tornadoes in urban areas almost always are verified while some weak tornadoes in rural areas may not be reported (Brotzge and Erickson 2010).

Results regarding impacts of distance from the radar indicated that the tornado to radar distances had little impact on lead time, but a significant impact on whether or not a warning was issued. Tornadoes are about 4.7% more likely to remain unwarned when located 100 km or more from a WSR-88D compared to those tornadoes located within 100 km of a radar (Brotzge and Erickson 2010). The impacts of tornado order and number per day revealed that for solitary tornado events (days with only one tornado), over half of all tornadoes were not warned. The first tornado of the day had a 44% chance of not being warned compared with a rate of about half that for the second (Brotzge and Erickson 2010). It's also important to note that some tornadoes may occur where there is less infrastructure to hit, resulting in a low F scale rating and a possibility of underestimating the tornado's actual strength.

Unfortunately, those tornadoes most likely to strike when the public is least likely to be aware are also those tornadoes with the greatest chance of not being warned. Those tornadoes occur during the night, during nonpeak tornado months of the year, and during nonoutbreak events (Brotzge and Erickson 2010).

2.3 Smith et al. (2012) and Thompson et al. (2012)

Smith et al. (2012) and Thompson et al. (2012) study convective modes for significant severe thunderstorms with a focus on tornadoes and severe reports (significant hail/wind gusts) because these events threaten life and property. Significant hail (sighail) events were defined as reports of hail with a diameter greater than or equal to 2 in., and significant wind (sigwind) events were classified by convective wind gusts greater than or equal to 65 kts.

All tornado, sighail, and sigwind reports for the period of 2003-2011 were filtered for the largest magnitude report per hour on a RUC model analysis grid with 40-km horizontal grid spacing (Smith et al. 2012). After filtering the data, 22 901 severe thunderstorm grid-hour events were produced, including 10 753 tornadoes, 4653 sighail, and 7495 sigwind. Archived level II WSR-88D data from NCDC (<http://www.ncdc.noaa.gov/nexradinv/>) were utilized from the closest radar site to an event (up to 230 km) to assign one of the following major convective mode classes for each severe thunderstorm event: Quasi-Linear Convective System (QLCS), supercell, and disorganized (cells/clusters) (Smith et al. 2012).

Part I of this study (Smith et al. 2012) assigned a convective mode to each case via manual examination of full volumetric radar data. The primary findings of this study are as follows: 1) discrete and cluster right-movers (RMs) were relatively more common as EF-scale damage ratings increased, 2) weak mesocyclones were most common with weak tornadoes, while 90% of EF3-EF5 tornadoes were associated with strong mesocyclones, 3) discrete RM tornado events were proportionally more common across

the high plains, with a transition eastward to higher relative frequencies of tornadoes with linear convective modes across the Mississippi and Ohio Valleys, 4) tornado events from linear convective modes were nearly as frequent in winter months as the sum of the discrete and cluster RM tornado events, 5) RM tornado events were most common across the interior northern Gulf coast during the winter, expanding across the Deep South and into the central Great Plains during the spring, northward into the northern Great Plains and Midwest during the summer, and then back southward into the lower Mississippi valley during the fall, and 6) QLCS tornado events displayed a notable eastward displacement away from the Great Plains toward the Mississippi and Ohio Valleys during the spring and summer (Smith et al. 2012). The majority of tornadoes occurred with discrete and cluster RMs compared to the QLCS and disorganized modes. More than 95% of EF3-EF5 tornadoes and sighthail events were produced by supercells (Smith et al. 2012).

Part II of this overall study (Thompson et al. 2012) examines relationships between severe thunderstorm events, convective mode, and environmental conditions using SPC hourly mesoanalysis data. The same dataset as Smith et al. (2012) was used. The derived parameters from the SPC mesoanalysis system were determined for each severe weather report and associated convective mode, forming the equivalent of a large close proximity sounding database for known storm types and severe weather events (Thompson et al. 2012). The convective modes and environments associated with the tornado events were the focus of Thompson et al. (2012).

Results by Smith et al. (2012) revealed that RM supercells dominated tornado production, thus forming the core of the investigation by Thompson et al. (2012). The

supercell composite parameter, as well as its constituent components effective storm relative helicity (ESRH) and effective bulk wind difference (EBWD), discriminated well between the disorganized tornadic storms and the three classes of supercells (discrete, cluster, line) (Thompson et al. 2012). The effective-layer significant tornado parameter (STP) and its components were also examined in seasonal comparisons of significant tornado RMs and EF1+ tornadic QLCS events. Despite the overall tendency for vertical shear parameters to discriminate well between tornadic and nontornadic supercells, vertical shear magnitude in the winter provided little insight into the differences between significant tornadic RMs and QLCS tornado events. Despite the relatively small values compared to spring and summer, mean layer convective available potential energy (MLCAPE) in the winter best differentiated between the QLCS tornadoes and significant tornadic RM events. During other seasons, deeper-layer (0-6-km BWD and EBWD) and low-level vertical shear (0-1-km SRH and ESRH) tended to be smaller for QLCS tornadoes compared to significant tornadic RMs (Thompson et al. 2012). The convective mode database used in both Smith et al. (2012) and Thompson et al. (2012) continues to be expanded upon on a yearly basis.

2.4 Tornado Probability of Detection and Lead Time using Convective Mode and Environmental Parameters

The research of Brotzge et al. (2013) evaluates two years of NWS tornado warnings, verification reports, and radar-derived convective modes across the CONUS to evaluate the ability of the NWS to warn on tornadoes across a variety of convective modes and environmental conditions. Two databases were used in their study. The first consisted of all tornado events and NWS warnings issued between 2000 and 2004

obtained from the Performance Branch of the NWS. A total of 18 763 tornado warnings and 7019 tornadoes were recorded during the five-year period. All data were county based, meaning if a tornado crossed the county line into a different county, it was counted as two separate events. The second database consisted of tornado and significant severe events between 2003 and 2011 compiled by the SPC (Brotzge et al. 2013). Their research was limited to the two-year overlap of the two databases; yielding a total of 2502 tornadoes with 9177 county-based warnings.

The results of Brotzge et al. (2013) confirmed their three hypotheses: 1) tornadoes from supercell storms were much easier to warn for in terms of POD and lead time than tornadoes from either QLCS or more disorganized, nonsupercell storms, 2) storm parameters including F-scale intensity and radar distance had a quantitatively significant impact on tornado POD and lead time, but varied as a function of storm morphology, and 3) the stronger, more intense storms, as determined by mesocyclone strength, MLCAPE, and vertical wind shear, had much higher tornado PODs and lead times than did weaker storms. Results point to lower tornado detection rates and shorter lead times associated with nonsupercell storms, weaker tornadic systems, and storms far from the radar and in higher populated areas (Brotzge et al. 2013).

2.5 Warning Decision Support System – Integrated Information

Lakshmanan et al. (2007) focus on the real-time, multi-radar applications and their utility for severe weather forecasting. The earliest version of the Warning Decision Support System (WDSS) was based on data from single radar. Since the development of WDSS, technological advances such as computer networking and compression methods

have made it possible to transmit data from multiple radars. Instead of only acquiring data from the nearest individual radar, one has access to a network of observing platforms.

Warning Decision Support System-Integrated Information (WDSS-II) provides a common data-access infrastructure, a suite of multisensory applications, and an extensible 4D visualization system (Lakshmanan et al. 2007). All data produced are in self-describing, extensible formats called Network Common Data Form (NetCDF). The system creates diagnostic products using automated algorithms. The first level of applications, such as *ldm2netcdf* and *ltgIngest*, are data ingest applications. Other applications provide meteorological products derived from a single source (Lakshmanan et al. 2007). Lakshmanan et al. (2007) surveyed forecasters on the usefulness of WDSS-II multisensory applications and display tools. The feedback related to this work includes the effectiveness of using multisensory applications to fill gaps in radar coverage and applications that provide information about the spatial extent of severe weather to reduce false alarm areas (both points are fundamental in using WDSS-II for this research).

The WDSS-II *w2merger* routine is a tool used to combine data from multiple radars on to a common grid. Using data from more than one radar improves geometry accuracy (such as cone of silence, beam spreading, beam height, beam blockage, etc.). Lakshmanan et al. (2006) used intelligent agents as a means to address the merger of scalar (such as reflectivity) and vector (such as velocity-wind field) data. These intelligent agents are computational systems that inhabit some complex dynamic environment, sense and act autonomously in this environment, and by doing so realize a set of goals or tasks for which they are designed (Lakshmanan et al. 2006).

The U.S. WSR-88D radar network has been updated to dual-polarization, giving NWS forecasters more information. The dual-polarized NWS radars transmit pulses of electromagnetic radiation that are polarized both horizontally and vertically. When these pulses reach a target, whether meteorological or non-meteorological, energy is scattered back to the radar. By comparing the signals received from returns at each polarization, one can glean information about the size, shape, and orientation of targets within the radar sampling volume (Kumjian, 2013).

Prior to this upgrade, conventional radars operated with a single, horizontal polarization. With dual-polarization, meteorologists gain access to more radar variables by comparing the returns in the horizontal and vertical; differential reflectivity (Z_{DR}), differential phase shift (Φ_{DP}), specific differential phase (K_{DP}), and cross correlation coefficient (ρ_{HV} or CC).

The research of Lack and Fox (2012) attempted to show the benefits of combining radar observations with Near-Storm Environment (NSE) information in order to produce a more accurate method of storm type classification. The four storm type classifications were supercell, linear, pulse, and unorganized. After storms were identified, individual cells within the storm system are selected based a minimum reflectivity threshold. These cells are assigned a number from 1 to the maximum number of cells identified and then storm attributes are derived for each (Lack et al. 2012). The overall objective of Lack and Fox (2012) was to use a classification tree to predict the classification of a storm based on its characteristics compared to a prior set of known classifications with similar characteristics. This study used WDSS-II, the aforementioned *w2merger* routine, and the

minimum reflectivity threshold concept to identify to tornadic cell and evaluate its associated radar variables.

2.6 Preliminary Study

The author completed previous isolated tornado research in 2014 that led to this deeper analysis. A data set of tornado events from the state of Kansas, 2004 to 2014, and their associated atmospheric parameter values was received from previous work done by Richard Thompson at the Storm Prediction Center (SPC). A tornado event was considered isolated if it was the only event within three days of any other tornado event. From this criterion, 50 tornado events remained from the original data set. These 50 events were compared to the SPC watch archive to match each event with its corresponding issued watch, if one was issued. 31 data points were NO WATCH events and the remaining 19 represented WATCH events. The parameters from Thompson that were subject to a 2-tail t-test included indicators of convective instability, thermodynamics and wind shear.

The results revealed that the parameters statistically significant at a 95% confidence level between WATCH and NO WATCH events were wind shear from surface to 1 km, surface to 3 km, surface to 6 km, and storm relative helicity (SRH) from the surface to 1 km and surface to 3 km. The Rapid Update Cycle Version 2 was used to construct a mean skew-T for both WATCH and NO WATCH scenarios. Comparison of the skew-T's showed that WATCH events had a small moisture slot and greater near surface wind shear.

CHAPTER 3: METHODOLOGY

3.1 Data Sorting

A data set of tornado events across the CONUS from 2004 to 2015 was obtained via e-mail correspondence with Richard Thompson at the SPC. The data consisted of the latitude, longitude, date and time of each tornado event as well as associated thermodynamic and kinematic parameters as a result of previous research done by Smith et al. (2012) and Thompson et al. (2012). Each tornado event is the maximum F-scale/EF-scale rating per hour on a 40 km horizontal grid utilizing RUC-II analysis. Convective mode for each tornado event was included, along with the nearest grid point value of many SPC mesoanalysis parameters (Thompson, personal communication). The data set was sorted by date and condensed to only include events after 2013 to ensure use of dual-polarization radar. The data were sorted by month and reduced to the months of April through September – as these months are primarily within the perceived “tornado season”. Lastly, the data were sorted by state and further reduced to events occurring in the geographic region between the Rocky and Appalachian mountain ranges. In summary, this dataset was overall reduced to only include years 2013-2015, months April – September, and states inside the Rocky and Appalachian mountain ranges.

All events were then manually evaluated one-by-one using NOAA’s archived Interactive Radar Map Tool (<https://gis.ncdc.noaa.gov/maps/ncei/radar>). The date and time of each event were set into the National Reflectivity Mosaic section. Tornadoes that were involved in outbreaks or large-scale events were not evaluated in this research and

were deleted from the dataset. Since this study focuses on isolated events, only tornadoes that occurred in a localized, isolated cell were considered. These tornadoes also needed to be the only tornado that formed out of that isolated cell.

The events were then analyzed using the Iowa Environmental Mesonet (IEM) “Search for NWS Watch/Warning/Advisories Products by County/Zone or by Point” to find whether or not a tornado warning was issued. The latitude/longitude of each event were put into the search, which resulted in a list of severe weather warnings, watches, and advisories for that area. Clicking on a tornado warning event for the specific date being analyzed would bring up a GIS map of the polygon warning area, a location marker of confirmed tornado, and the start and end of the warning. Simultaneously, each event was double-checked with the NOAA storm archive database to ensure it was reported. This left the dataset with 39 isolated tornadoes that occurred with a positive lead-time warning from the NWS and 57 that were not warned for at all. Each WARN and NOWARN event were then paired together by similar geographic location and time to reduce bias, leaving 33 of each event (Table 3.1). These pairs were determined by sorting the dataset based on whether or not a warning was issued. If a NOWARN and WARN event occurred close to each other in geographic location, time of day, and month, they were “paired” together and kept in the dataset. This was believed to reduce bias because we want do not want significant differences in environment (based on geographic location), seasonality (based on month), and effects of day-time heating (based on time of day). Again, NOWARN classifies an isolated cell that spawned one single tornado that was not warned for by the NWS, and WARN classifies an isolated cell that spawned one single tornado that was warned for by the NWS. A Student’s t-test was performed on the thermodynamic and

kinematic parameters to test their significance between warned and unwarned isolated tornadoes.

Table 3.1 Excel workbook of isolated tornadoes after completed data sorting. From left to right: date time, Weather Forecasting Office (WFO), whether or not warning was issued (Y = Yes, N = No), F-scale magnitude, state, distance tornado occurred from the WFO, latitude, and longitude. These events and their associated parameters were found by utilizing RUC-II analysis soundings.

date	time	WFO	Warning?	magnitude	state	WFO dist	slat	slon
5/8/2013	19:54	KGLD	N	0	CO	154.274	38.1	-102.43
5/8/2013	22:00	KFSD	N	0	SD	72.46	43.1	-97.35
5/17/2013	19:45	KHTX	Y	0	AL	72.8014	34.95	-86.88
5/17/2013	21:54	KUDX	Y	0	NE	157.195	42.78	-103.4
5/18/2013	22:58	KCYS	Y	0	NE	176.528	41.73	-102.85
5/18/2013	0:50	KDYX	Y	1	TX	67.9544	33	-98.78
5/27/2013	0:23	KDMX	Y	0	IA	118.208	40.79	-94.37
5/29/2013	2:06	KFDX	Y	0	TX	76.3244	34.99	-102.92
5/31/2013	23:09	KARX	N	0	IA	144.263	43.17	-92.73
6/5/2013	22:42	KMPX	N	0	MN	88.2814	44.18	-92.97
6/14/2013	14:50	KDFX	N	0	TX	54.2166	29.33	-99.73
6/19/2013	22:45	KLBB	Y	2	TX	72.0524	33.48	-102.56
6/26/2013	4:25	KMVX	Y	0	MN	120.216	46.65	-96.42
7/9/2013	20:54	KBIS	N	0	ND	42.0417	46.91	-101.26
7/13/2013	0:45	KABR	Y	0	ND	107.163	46.06	-97.35
7/20/2013	23:26	KLNX	N	0	NE	161.899	42.6	-102.34
7/22/2013	0:18	KSGF	N	0	MO	10.3862	37.21	-93.27
7/23/2013	21:22	KPBZ	Y	0	OH	63.6374	40.69	-80.94
7/30/2013	21:35	KUDX	N	0	SD	89.9088	44.03	-101.72
8/1/2013	21:42	KLBB	N	0	TX	1.44077	33.66	-101.83

8/7/2013	21:48	KLBB	N	0	TX	24.2066	33.53	-102.02
8/11/2013	20:36	KUDX	Y	1	SD	65.9794	43.9	-103.59
8/27/2013	1:15	KMVX	Y	0	MN	203.859	46.46	-95.16
8/31/2013	0:10	KBIS	Y	0	ND	57.8548	46.88	-101.49
5/6/2014	20:07	KRIW	N	1	WY	27.6436	43.2966	-108.34
5/14/2014	20:30	KCYS	N	0	NE	166.466	42.07	-103.24
5/22/2014	1:15	KCYS	Y	0	WY	117.9	42.2021	-105
5/25/2014	18:45	KMAF	Y	0	TX	185.47	30.3808	-102.87
5/31/2014	19:34	KRIW	N	0	WY	128.726	43.34	-110.01
6/3/2014	18:07	KRIW	N	0	WY	84.1535	43.7665	-108.86
6/14/2014	23:11	KFTG	Y	0	CO	90.9617	39.56	-103.53
6/23/2014	0:06	KFTG	N	0	CO	77.6736	40.4	-104.12
6/25/2014	20:00	KMKX	Y	0	WI	76.9783	42.74	-89.44
7/2/2014	22:00	KDYX	N	0	TX	71.6244	33.1018	-99.613
7/27/2014	19:29	KILN	Y	0	OH	78.2903	40.1236	-83.613
8/7/2014	0:10	KFTG	N	0	CO	11.4353	39.76	-104.42
8/12/2014	15:15	KILN	N	0	OH	129.573	40.1753	-82.632
9/17/2014	20:38	KSGF	Y	0	AR	142.994	35.9894	-92.966
9/30/2014	21:45	KABR	Y	0	SD	81.2898	45.89	-99.25
4/8/2015	20:30	KLSX	Y	1	MO	84	37.9446	-90.799
4/11/2015	23:36	KAMA	Y	0	TX	36	35.539	-101.69
4/12/2015	1:06	KDDC	Y	0	KS	139	37.33	-101.44
4/17/2015	23:55	KGLD	Y	0	KS	28	39.17	-101.5
4/23/2015	23:51	KGLD	Y	1	CO	174.417	40.8229	-102.47
4/24/2015	20:37	KDYX	Y	1	TX	78	31.9865	-99.778
5/3/2015	22:34	KFSD	N	0	IA	150.419	43.31	-94.93
5/5/2015	20:23	KMAF	Y	1	TX	83	32.4493	-101.55

5/13/2015	22:57	KLBB	N	0	TX	137.423	33.6231	-100.34
5/15/2015	21:34	KCYS	Y	1	WY	99	41.919	-104.21
5/15/2015	1:20	KEAX	N	0	MO	129.972	39.5878	-93.135
5/22/2015	23:13	KMAF	N	0	TX	202.416	30.4802	-103.46
5/26/2015	23:32	KTLX	Y	0	OK	123.618	35.5213	-98.625
5/29/2015	15:40	KDGX	N	0	MS	135.818	33.3874	-90.611
6/15/2015	22:16	KCYS	N	0	WY	132	41.9	-106.04
6/20/2015	2:57	KUDX	Y	2	SD	34	44.417	-103.01
6/23/2015	17:39	KILN	N	0	OH	106.186	39.6984	-82.613
7/7/2015	21:30	KRIW	N	0	WY	157.771	41.6651	-108.16
7/12/2015	3:24	KMBX	Y	0	ND	97.3328	48.15	-99.61
7/13/2015	23:33	KARX	N	0	WI	107	43.1812	-90.196
7/17/2015	1:34	KARX	N	0	IA	155.038	43.2575	-92.941
7/24/2015	23:40	KMPX	N	0	MN	139	43.8908	-94.69
8/9/2015	20:35	KFSD	Y	0	SD	138.543	43.81	-98.44
8/9/2015	1:55	KOAX	N	1	NE	121	40.2576	-96.013
8/16/2015	21:59	KFTG	Y	0	CO	68.6637	40.4	-104.49
8/28/2015	23:40	KICT	N	0	KS	38.3896	37.96	-97.24
9/11/2015	1:16	KTWX	N	1	KS	25	38.9099	-95.967

3.2 WDSS and MatLab

RADAR Level-II base data were ordered from NOAA's NEXRAD archive.

These were downloaded and processed using WDSS-II and the previously mentioned

w2merger routine. The *w2merger* routine processed reflectivity, azimuthal shear,

divergence, spectrum width, Zdr, and RhoHV for each event based on specific radar

locations (the radar closest to each event). NEXRAD radars have a maximum range of

250km, however, this script that processed the radar level-II base data only processed data at a range of 150km. This created an issue with sample size. Some events occurred outside the cutoff and were eliminated from the radar analysis, reducing WARN to 19 events and NOWARN to 16 events (Table 3.2). On the other hand, this is believed to be better for the analysis and discussion because the radar beam misses the lower 2 km of the atmosphere beyond 150km range. This will better represent the tornadic atmosphere as tornadoes occur within the lowest 2 km of the atmosphere, although sample size was sacrificed. Expanding the dataset will be discussed in chapter five with future work.

Table 3.2 Excel workbook of isolated tornado events within 150km range of radar, sorted by date.

date	WFO	Warning?	time
5/8/2013	KGLD	N	19:54
5/8/2013	KFSD	N	22:00
5/31/2013	KARX	N	23:09
6/5/2013	KMPX	N	22:42
6/14/2013	KDFX	N	14:50
7/9/2013	KBIS	N	20:54
7/30/2013	KUDX	N	21:35
8/1/2013	KLBB	N	21:42
5/6/2014	KRIW	N	20:07
7/2/2014	KDYX	N	22:00
8/7/2014	KFTG	N	0:10
8/28/2015	KICT	N	23:40
9/11/2015	KTWX	N	1:16
8/12/2014	KILN	N	15:15
7/13/2015	KARX	N	23:33
8/9/2015	KOAX	N	1:55
5/17/2013	KHTX	Y	19:45
5/18/2013	KDYX	Y	0:50
6/19/2013	KLBB	Y	22:45
6/26/2013	KMVX	Y	4:25
7/13/2013	KABR	Y	0:45
7/23/2013	KPBZ	Y	21:22
8/11/2013	KUDX	Y	20:36
8/31/2013	KBIS	Y	0:10
6/14/2014	KFTG	Y	23:11
6/25/2014	KMKX	Y	20:00
7/27/2014	KILN	Y	19:29
9/30/2014	KABR	Y	21:45
4/8/2015	KLSX	Y	20:30
4/11/2015	KAMA	Y	23:36
4/17/2015	KGLD	Y	23:55
5/5/2015	KMAF	Y	20:23
6/20/2015	KUDX	Y	2:57
5/26/2015	KTLX	Y	23:32
7/12/2015	KMBX	Y	3:24

Once processed and saved to their own folder based on date, the data were loaded and unzipped in MatLab. A MatLab code, from here on referred to as “*CellVort*” (listed in Appendix), was written to pick out individual cells and associated radar variables. This code analyzes the radar data based on a reflectivity threshold. *CellVort* was run for each event with a reflectivity threshold that was case specific. If a tornadic cell was embodied in a widespread precipitation event, the threshold was increased to pick out the specific cell/area of the cell that the tornado occurred. This was done to ensure that the values of the radar parameters were specific to the tornado and not the overall cell. Each run resulted in a reflectivity composite side-by-side with the results of the individual cells that were picked out by *CellVort* (Figures 3.1, 3.2, 3.3, and 3.4).

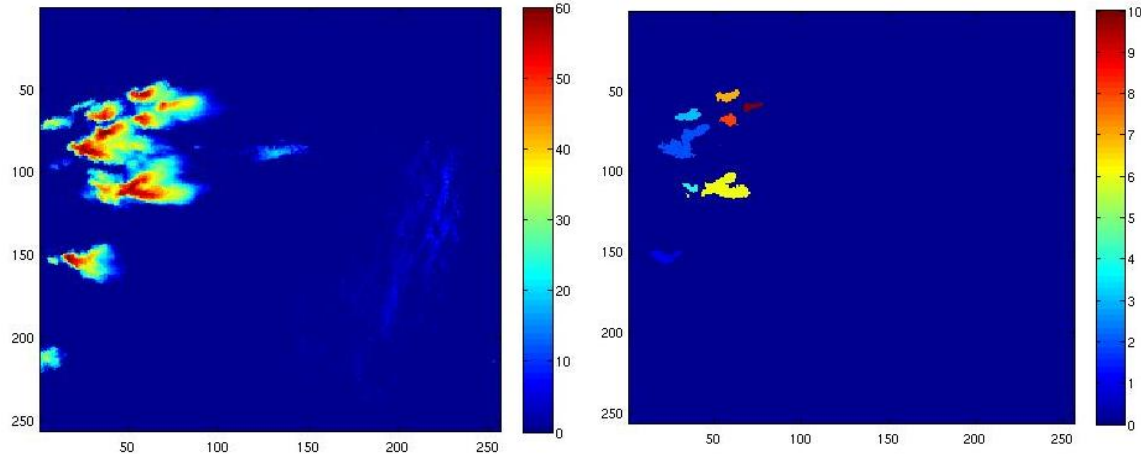


Figure 3.1 *CellVort* imagery result for event 20130831 prior to tornado formation. The yellow cell is the tornadic cell (assigned reference number 6). This event did receive a NWS warning.

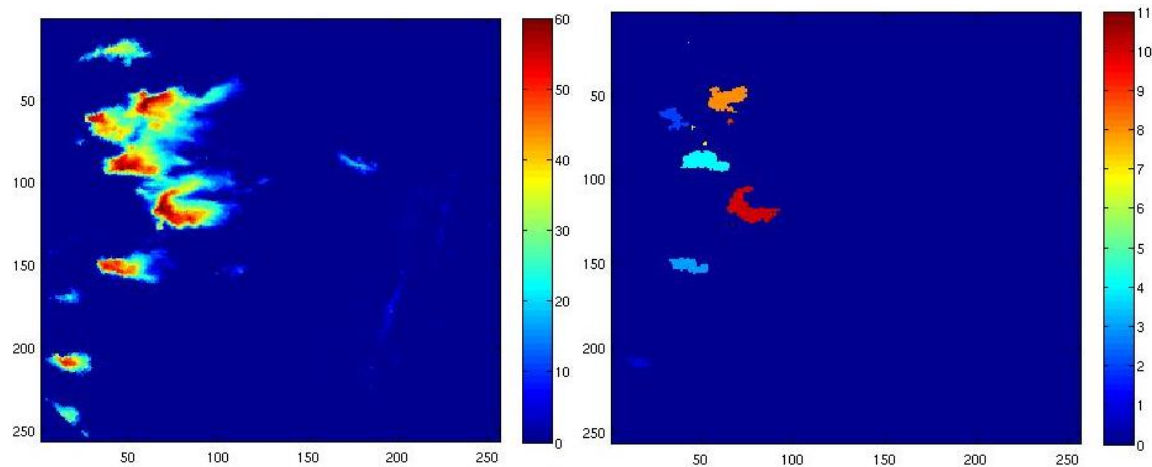


Figure 3.2 Time of tornado (WARN) *CellVort* imagery result for event 20130831. The dark red cell is the tornadic cell (assigned reference number 10).

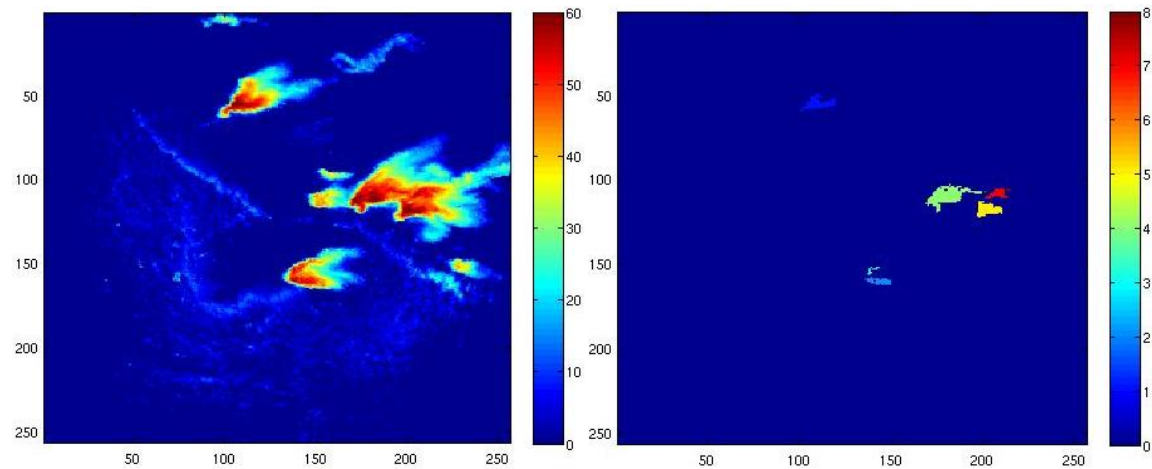


Figure 3.3 *CellVort* imagery result for event 20130730 prior to tornado formation. The yellow cell is the tornadic cell (assigned reference number 5). This event did not receive a NWS warning.

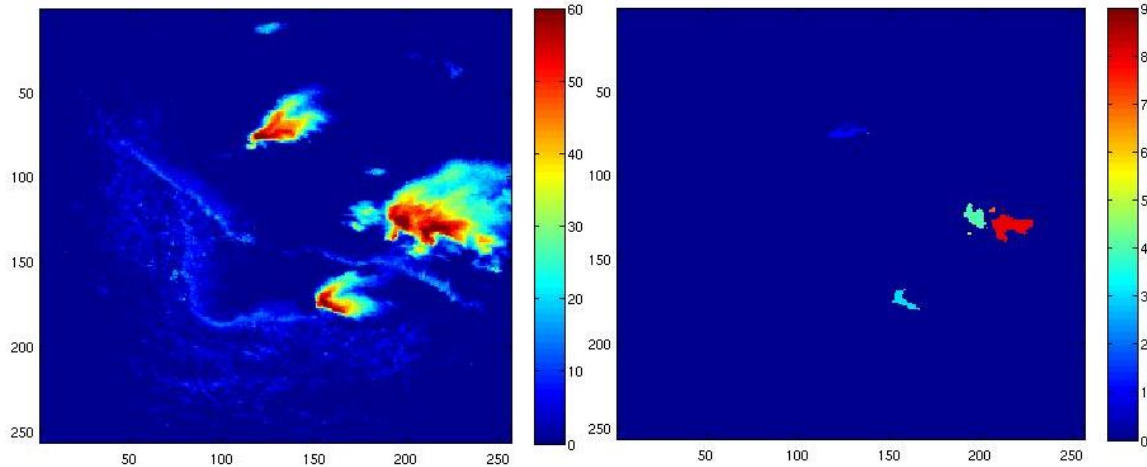


Figure 3.4 *CellVort* imagery result for event 20130730 (NOWARN) at time of tornado formation. The red cell is the tornadic cell (now assigned reference number 8).

Each cell was assigned a reference number to be found in “zstructure” (an excel-like format with parameter value results for each cell from each time step). The reference number could be found by matching the color of the cell to the color bar on the right hand side, or using the x and y axis on the grid that can be matched to the results listed in zstructure. The x and y axes represent distances in km with the radar location at the center of the grid. A list of times from the resulting *CellVort* run would appear in zstructure. Clicking on a specific time (i.e. time before tornado formation or time of tornado formation) would bring up another excel-like format worksheet with parameter values and cell reference number. Matching the cell reference number within zstructure to the cell number that was given to the tornadic cell in the imagery would result in values for each parameter that was tested. The radar variables examined were azimuthal shear (maximum, minimum and mean), azimuthal shear below 3km (maximum, minimum and mean), divergence (maximum, minimum, and mean), maximum echo top, rhoHV (minimum and mean), and spectrum width (maximum and mean). These variables

were chosen because they are the most representative of tornado formation when forecasting tornadoes using radar imagery.

Data from each variable were collected for the time of tornado occurrence and 30 minutes prior to formation because the NWS goal for 2025 is to have a 45 minute lead-time for tornadoes. The values of the radar parameters were copied from the *CellVort* analysis results located in zstructure into their own excel worksheets. Time before tornado WARN vs. NOWARN and time of tornado WARN vs. NOWARN had their own separate excel workbooks and the tabs in each were labeled with the parameters tested and their values. A Student's t-test was then run between WARN and NOWARN events for all variables collected from *CellVort* results at time of tornado and 30 minutes before.

At this time, another hypothesis arose; is there a significant difference among those tornadic cells that were accurately warned for compared to the surrounding cells that were not tornadic and did not receive a warning? What did the forecaster see in this one cell versus the surrounding others that urged them to issue a warning? To explore this, *CellVort* was used again to evaluate the surrounding nontornadic cells of the WARN events (NTC). Although some WARN events were single-cell, 10 events occurred in a “cluster” environment. To ensure the surrounding cells (NTCs) did not receive a false alarm or an overlapping warning polygon, the events were reevaluated using the same IEM search as before.

A two-tailed, two-sample equal variance Student's t-test was performed on the following: Time of tornado thermodynamic and kinematic parameters (Table 4.1), 30 minutes before tornado formation WARN vs NOWARN (Table 4.2), time of tornado

formation WARN vs NOWARN (Table 4.3), time of warning WARN vs NTC (Table 4.4), time of tornado formation WARN vs nearby NTC (Table 4.5), and time of tornado formation NOWARN vs NTC (Table 4.6). Testing was done for equal variances to determine whether there is a difference between the two groups. The resulting p-values and means are listed in each corresponding table. A 90% confidence interval was used for analysis due the extremity of the results – most p-values were exceptionally large.

CHAPTER 4: RESULTS and DISCUSSION

4.1 Thermodynamic and Kinematic Parameters at Time of Event

Thermodynamic and kinematic parameters which show a difference between the WARN and NOWARN cases at 90% confidence level are listed in Table 4.1. These were the parameters included in the dataset provided by Richard Thompson and are at time of tornado formation. The parameters tested were: MLCAPE, MUCAPE, SBCAPE, CAPE 0-3km, MLLCL, MULCL, MULFC, Surface Temperature, Surface Dewpoint Temperature, MLCIN, MUCIN, SBCIN, Lapse Rate 0-3km, Lapse Rate 700-500mb, Lapse Rate 850-500mb, Wind Shear 0-6km, Wind Shear 0-3km, Wind Shear 0-1km, SRH 0-1km, SRH 0-3km, Precipitable Water, Surface Relative Humidity, Significant Tornado Parameter. Only the parameters that tested statistically significant are listed.

Table 4.1 P-values and means for thermodynamic and kinematic parameters at time of tornado between WARN and NOWARN. Parameters highlighted are those that are statistically significant at 95% confidence interval.

Parameter	NOWARN Mean	WARN Mean	P-Value
Mean Layer CIN	-17.73	-37.5	0.047205
Surface Based CIN	-24.17	-49.11	0.098783
Lapse Rate 0-3 km	7.51	6.93	0.073726
Shear 0-6 km	33.90	43.36	0.002484
Shear 0-3 km	23.60	28.38	0.041003
Shear 0-1 km	9.99	13.09	0.087542
Storm Relative Helicity 0-1 km	50.91	86.65	0.030818
Storm Relative Helicity 0-3 km	108.98	172.82	0.002746
Significant Tornado Parameter	0.36	0.64	0.079722

As expected, shear at all three levels provided were seen to be statistically significant. The average value of shear 0-6 km for NOWARN was 33.90 m/s and 43.36 m/s for WARN, and of shear 0-1 km for NOWARN was 9.99 m/s and 13.09 m/s for WARN. The isolated tornadoes that received a NWS warning possessed a greater wind shear at all levels of the atmosphere and were more likely easier to depict for tornado formation.

With shear at higher levels of the atmosphere (0-3km and 0-6km) being more statistically significant than low level shear (0-1km), it appears that maybe an upper level jet gave way to the accurate forecasting of WARN events. The events were then reanalyzed again using the IEM search to look for associated watches issued before the warning. If a watch was issued before the warning, it is implied that large scale motions (such as the upper level jet) may have given the forecaster more confidence in issuing the warning. Only 7 of 33 WARN events received a tornado watch prior to tornado warning, and 19 of the 33 received a severe thunderstorm warning prior to tornado warning, leaving only 7 events that had no prior warning before the tornado warning was issued. It is also important to note that the majority of WARN events had several false alarm tornado warnings issued before and after the actual accurate warning was issued. This implies that forecasters were well aware of the tornadic potential of these events prior to tornado formation.

According to the SPC definition of SRH, larger values of 0-3 km SRH (greater than $250 \text{ m}^2/\text{s}^2$) and 0-1 km SRH (greater than $100 \text{ m}^2/\text{s}^2$) suggest an increased threat of tornadoes and although larger values are generally better, there are no clear “boundaries” between non-tornadic and significant tornadic supercells. The results of this study show there is a significant difference between WARN and NOWARN when it comes to SRH. The average values of SRH 0-1 km and SRH 0-3 km for NOWARN were $50.91 \text{ m}^2/\text{s}^2$ and $108.98 \text{ m}^2/\text{s}^2$, respectively, and for WARN were $86.65 \text{ m}^2/\text{s}^2$ and $172.82 \text{ m}^2/\text{s}^2$, respectively. Although neither quite makes it to the “large” values as discussed by the SPC, there is a clear difference between the two.

The results show a significant kinematic difference between WARN and NOWARN, especially at the 95% confidence interval. Although the issuance of each warning, or lack thereof, is ultimately the decision and bias of the forecaster on duty, the NOWARN events do not appear to possess kinematic values that may be deemed threatening by the forecaster. Although these storms produced tornadoes, it is not surprising that forecasters did not warn under these conditions.

4.2 Radar Parameters – Warned vs. Unwarned

The results of the Student's t-test between WARN and NOWARN 30 minutes prior to tornado formation are listed in Table 4.2. At a 95% confidence interval, no parameters were statistically significant, but mean azimuthal shear at lowest altitude and minimum and mean azimuthal shear below 3-km were statistically significant at a 90% confidence interval. However, at a 95% confidence level, we can say WARN and NOWARN events 30 minutes prior to tornado formation appear to be very similar on radar imagery. With no clear indication 30 minutes prior to formation, but more apparent shear at time of formation, forecasters may need to combine radar imagery and environmental analysis to accurately warn on these cases.

Table 4.2 Resulting p-values from the Student's t-test comparison of before tornado formation between WARN and NOWARN. No results were significant at 95% confidence interval.

Parameter	NOWARN Mean	WARN Mean	P-Value
Minimum Azimuthal Shear at Lowest Altitude	-0.0057	-0.0066	0.344336368
Mean Azimuthal Shear at Lowest Altitude	0.000040	0.000094	0.060679261
Maximum Azimuthal Shear below 3km	0.0085	0.0095	0.542507749
Minimum Azimuthal Shear below 3km	-0.0042	-0.0056	0.082334836
Mean Azimuthal Shear below 3km	0.00031	0.00041	0.089377726
Maximum Divergence	0.0021	0.0023	0.290309457
Minimum Divergence	-0.0033	-0.0037	0.519808604
Mean Divergence	0.000013	-0.000000037	0.463785393
Maximum Echo Top	8.66	8.90	0.354408
Minimum RhoHV	0.52	0.40	0.32976052
Minimum RhoHV – without zeroes	0.70	0.75	0.522486
Mean RhoHV	0.98	0.98	0.93697
Maximum Spectrum Width	7.35	8.38	0.146375
Mean Spectrum Width	2.48	2.31	0.336657

Table 4.3 lists the p-value results of the Student's t-test performed between WARN and NOWARN at time of tornado formation. At a 95% confidence interval, mean azimuthal shear at lowest altitude, mean azimuthal shear below 3-km, and maximum spectrum width are statistically significant. The mean azimuthal shear at lowest altitude

and below 3-km relate to the results in Table 4.1 that determined shear and SRH at 0-3 km as statistically significant. It is becoming apparent that the main difference between WARN and NOWARN events take place in the lower 3-km of the atmosphere and are primarily shear related.

Table 4.3 Resulting p-values from the Student's t-test comparison at Time of Tornado between WARN and NOWARN as well as their associated means. Results statistically significant at a 95% confidence interval are highlighted.

Parameter	NOWARN Mean	WARN Mean	P-Value
Minimum Azimuthal Shear at Lowest Altitude	-0.0057	-0.0065	0.393204298
Mean Azimuthal Shear at Lowest Altitude	0.000012	0.000097	0.013982761
Maximum Azimuthal Shear below 3km	0.0092	0.010	0.456395509
Minimum Azimuthal Shear below 3km	-0.0046	-0.0049	0.637394941
Mean Azimuthal Shear below 3km	0.00031	0.00049	0.008311522
Maximum Divergence	0.0025	0.0031	0.334845996
Minimum Divergence	-0.0033	-0.0035	0.779326591
Mean Divergence	-0.000021	0.000018	0.138260908
Maximum Echo Top	8.66	8.84	0.517001
Minimum RhoHV	0.54	0.50	0.74449777
Minimum RhoHV – without zeroes	0.67	0.79	0.059386
Mean RhoHV	0.98	0.98	0.350295
Maximum Spectrum Width	7.57	9.01	0.018524
Mean Spectrum Width	2.77	2.50	0.57786

4.3 Radar Parameters – WARN vs. Nontornadic Cells

The next hypothesis that arose was to find any difference between the tornadic cells that received NWS warning and the nontornadic cells in the surrounding area of the WARN event. Results from the Student's t-test between the parameters from these two events at time of tornado warning are listed in Table 4.4. Statistically significant at a 95% confidence interval are the following: minimum azimuthal shear at lowest altitude, minimum azimuthal shear below 3-km, maximum and minimum divergence, and minimum RhoHV (excluding values of zero).

Table 4.4 Resulting p-values from the Student's t-test comparison of tornadic cell and nearby nontornadic cells at time of warning as well as the means. Results statistically significant at a 95% confidence interval are highlighted.

Parameter	NTC Mean	WARN Mean	P-Value
Minimum Azimuthal Shear at Lowest Altitude	-0.0040	-0.0073	0.000376192
Mean Azimuthal Shear at Lowest Altitude	0.000091	0.000089	0.944603975
Maximum Azimuthal Shear below 3km	0.025	0.011	0.381741427
Minimum Azimuthal Shear below 3km	-0.0034	-0.0062	0.000313903
Mean Azimuthal Shear below 3km	0.00041	0.00041	0.979507626
Maximum Divergence	0.0017	0.0024	0.000074961
Minimum Divergence	-0.0018	-0.0041	0.000132302
Mean Divergence	0.000018	0.000012	0.633470886
Maximum Echo Top	9.00	8.85	0.332195
Minimum RhoHV	0.28	0.98	0.38379892
Minimum RhoHV – without zeroes	0.84	0.74	0.022721
Mean RhoHV	0.98	0.98	0.505027
Maximum Spectrum Width	7.82	8.68	0.18706
Mean Spectrum Width	2.66	2.36	0.143515

Values of minimum azimuthal shear at lowest altitude ranged from -0.0074s^{-1} to -0.0025s^{-1} for the NTCs and from -0.0148s^{-1} to -0.0035s^{-1} for the WARN tornadic cell (Figure 4.1). It is evident here that not only does the tornadic cell have a slightly greater range in values, but also a more extreme minimum than the NTCs. The same statement is

relevant when comparing minimum azimuthal shear below 3-km (with almost identical box and whisker plots – not shown); the NTCs range from -0.006s^{-1} to -0.0022s^{-1} and the WARN range from -0.0117s^{-1} to -0.0029s^{-1} .

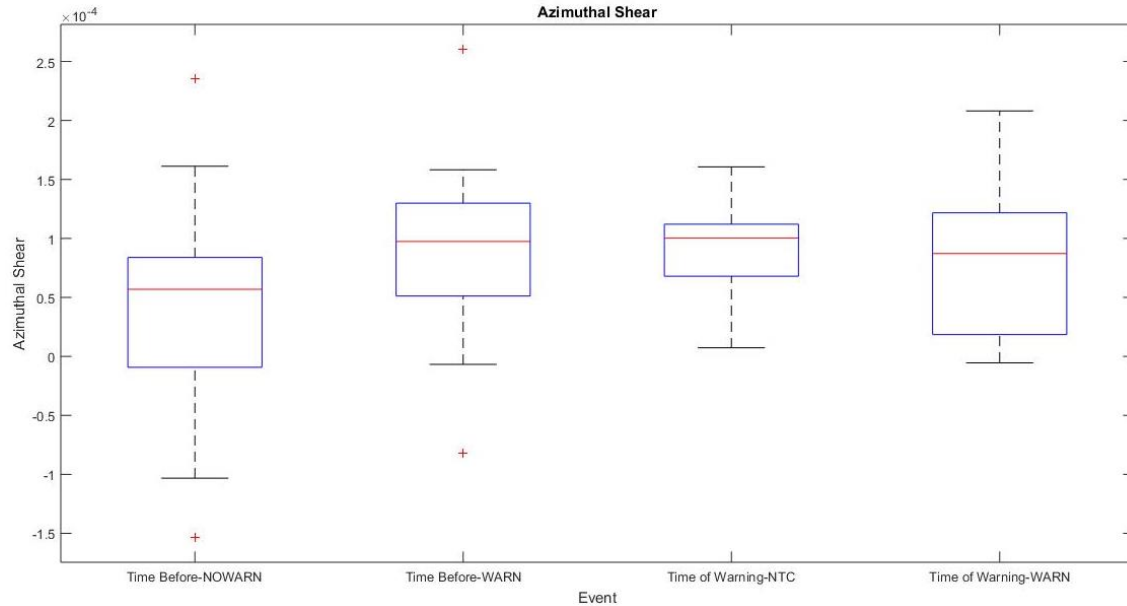


Figure 4.1 Box and whisker plots of azimuthal shear (s^{-1}) at time before tornado (NOWARN), time before (WARN), time of warning (NTC), and time of warning (WARN).

Overall, there seems to be an indicator of possible tornado formation when focusing on divergence (Figure 4.2) and convergence (Figure 4.3). The majority of the NTCs have very low values of divergence compared to the higher values of the WARN events. Although the range is similar, there are more large values ($\sim 0.0025\text{s}^{-1}$) with the WARN cells than the NTCs as well as NOWARN.

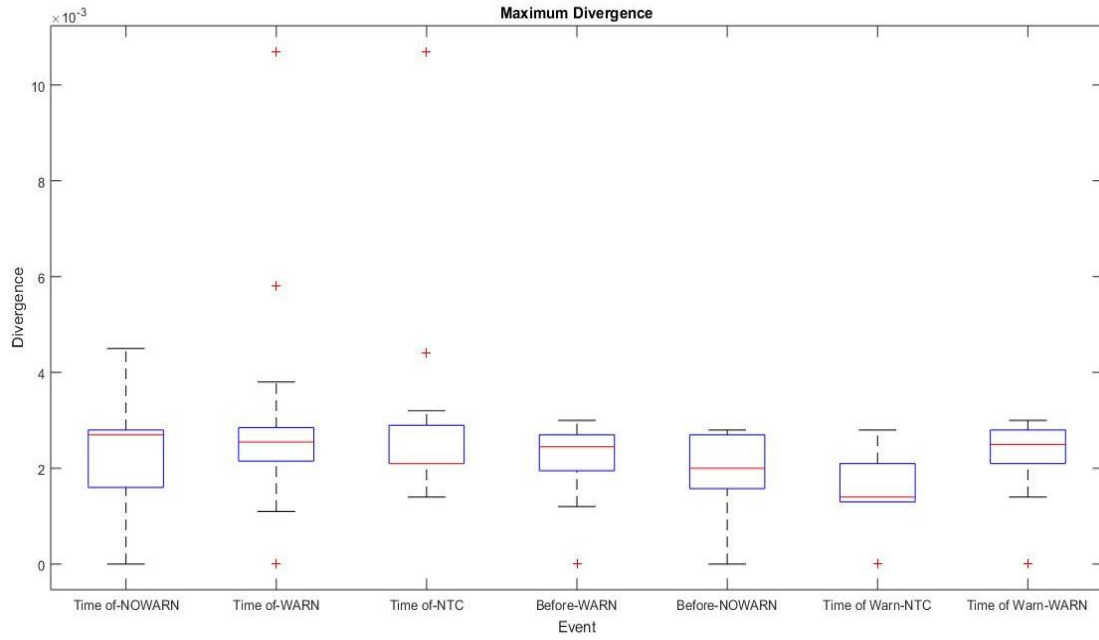


Figure 4.2 Box and whisker plots of maximum divergence (s^{-1}) among all time steps and events analyzed. From left to right: NOWARN at time of tornado formation, WARN at time of tornado formation, NTCs at time of tornado formation, WARN before formation, NOWARN before formation, NTC at time of warning, and WARN at time of warning.

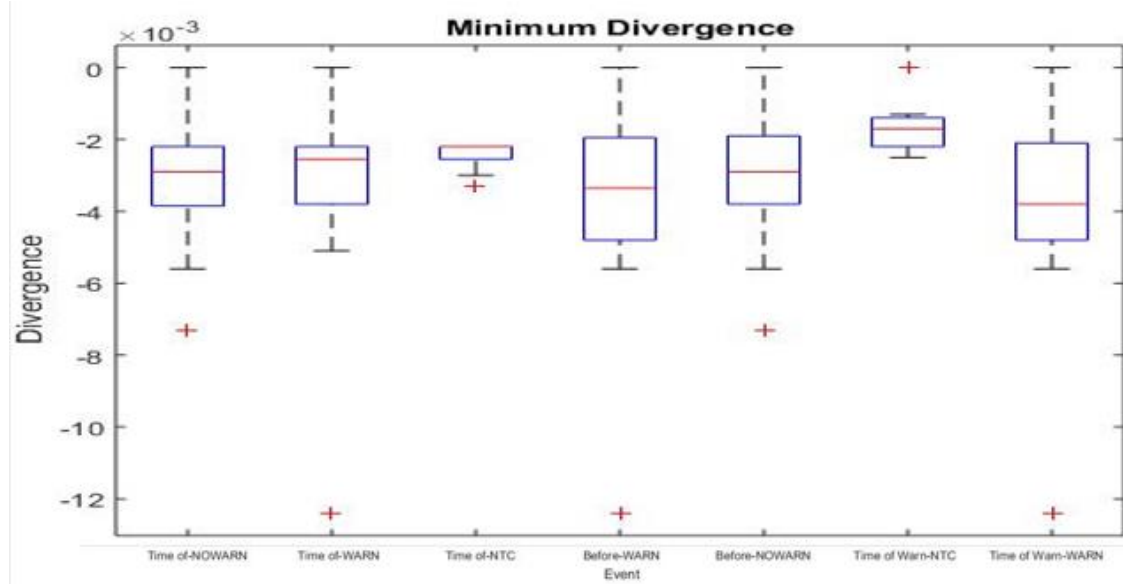


Figure 4.3 Box and whisker plots of minimum divergence (s^{-1}) (convergence) among all time steps and events analyzed. From left to right: NOWARN at time of tornado formation, WARN at time of tornado formation, NTCs at time of tornado formation, WARN before formation, NOWARN before formation, NTC at time of warning, and WARN at time of warning.

Only one radar parameter resulted as statistically significant at a 95% confidence interval between NTCs and WARN at time of tornado (Table 4.5); mean RhoHV. This is obvious and almost expected. NTCs had a higher value of mean RhoHV due to their uniform meteorological hydrometeors while WARN experienced slightly lower values, possibly due to tornadic debris. At time of warning (Table 4.4), azimuthal shear and divergence were statistically significant between WARN and NTC. Now at time of formation, only RhoHV shows as significant. These storms appear to have a similar morphology, but the tornadic cell possesses significant values of azimuthal shear and divergence prior to formation (at time of warning).

Table 4.5 Resulting p-values from the Student's t-test between tornadic cell and nearby nontornadic cells at time of tornado and their associated means. The one parameter statistically significant at a 95% confidence interval is highlighted.

Parameter	NTC Mean	WARN Mean	P-Value
Minimum Azimuthal Shear at Lowest Altitude	-0.0055	-0.0065	0.182371001
Mean Azimuthal Shear at Lowest Altitude	0.000075	0.000097	0.107172704
Maximum Azimuthal Shear below 3km	0.010	0.010	0.908580309
Minimum Azimuthal Shear below 3km	-0.0039	-0.0049	0.103919567
Mean Azimuthal Shear below 3km	0.00051	0.00049	0.64488444
Maximum Divergence	0.0030	0.0031	0.987691531
Minimum Divergence *	-0.0025	-0.0035	0.050206324
Mean Divergence	0.000025	0.000018	0.5190085
Maximum Echo Top	9.00	8.84	0.330565
Minimum RhoHV	0.69	0.50	0.08815684
Minimum RhoHV – without zeroes	0.83	0.79	0.163221
Mean RhoHV	0.9811	0.9779	0.016523
Maximum Spectrum Width	9.05	9.01	0.923193
Mean Spectrum Width	2.70	2.50	0.349843

4.4 Radar Parameters – NOWARN vs. Nontornadic Cells

Results thus far created the question: do NOWARN events appear to be similar to NTCs and therefore do not receive a warning? A Student's t-test was performed again, but this time between NOWARN events and the nontornadic cells. With several radar parameters resulting as statistically significant at a 95% confidence interval, it appears that NTCs and NOWARN are not similar; meaning, forecasters can accurately pick out which cell in a cluster will be tornadic and warn on it. However, when looking at Figure 4.4, it is evident that the NOWARN events have a more sporadic distribution of azimuthal shear values, making these specific environments difficult to assess for tornado potential.

Table 4.6 Resulting p-values from the Student's t-test comparing tornadic cells with no warning and nontornadic cells that occurred nearby the tornadoes with warnings, as well as their associated means. Results statistically significant at a 95% confidence interval are highlighted.

Parameter	NTC Mean	NOWARN Mean	P-Value
Minimum Azimuthal Shear at Lowest Altitude	-0.0055	-0.0057	0.759774569
Mean Azimuthal Shear at Lowest Altitude	0.000075	0.000012	0.033835825
Maximum Azimuthal Shear below 3km	0.010	0.0092	0.418866102
Minimum Azimuthal Shear below 3km	-0.0039	-0.0046	0.209031218
Mean Azimuthal Shear below 3km	0.00051	0.00031	0.001002209
Maximum Divergence	0.0030	0.0025	0.40571302
Minimum Divergence	-0.0025	-0.0033	0.017525974
Mean Divergence	0.000025	-0.000021	0.043426578
Maximum Echo Top	9.00	8.66	0.094654
Minimum RhoHV	0.69	0.54	0.15724449
Minimum RhoHV – without zeroes	0.83	0.67	0.015456
Mean RhoHV	0.9811	0.9753	0.010131
Maximum Spectrum Width	9.05	7.57	0.00008231
Mean Spectrum Width	2.70	2.77	0.878643

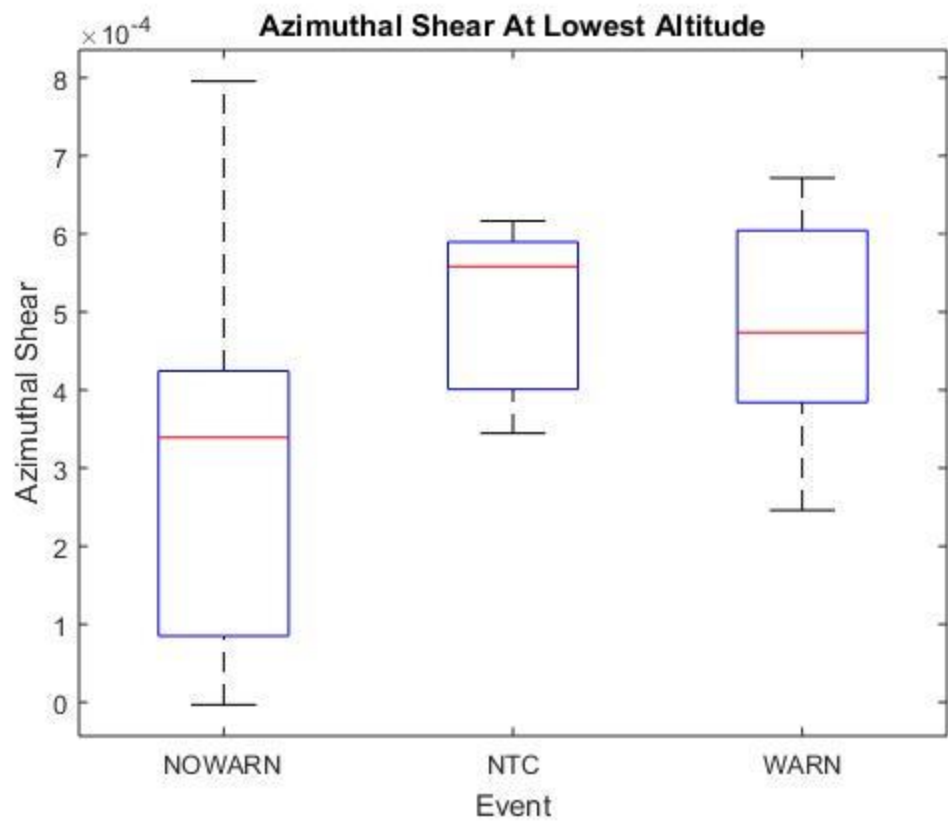


Figure 4.4 Box and whisker plots of azimuthal shear (s^{-1}) at time of tornado for NOWARN, NTC and WARN events.

CHAPTER 5: CONCLUSIONS

5.1 Conclusion

The purpose of this study was to understand what, if any, atmospheric parameters and RADAR variables are different between isolated tornadoes that are anticipated by NWS tornado warning and ones that are not warned. The hypothesis was that wind shear and azimuthal shear are statistically significant between isolated tornado events anticipated by a NWS warning (WARN) and isolated tornado events not anticipated by a NWS warning (NO WARN). More specifically, the authors believed that the unwarned tornadoes do not possess a noticeable value of shear and therefore do not represent a well-known tornadic precursor on RADAR imagery. Results from this research show this to be true. Shear, divergence, and convergence were statistically significant in several of the Student's t-test runs and may be something that forecasters want to focus on more when facing isolated cells.

However, the results displayed in Figure 4.1 and 4.4 reveal that azimuthal shear may not be a good indicator of isolated tornadic storms. There is no threshold value we can determine by looking at these results. The distribution is too sporadic and reaches values both above and below those within the NTCs. Azimuthal shear may have resulted as statistically significant, but it cannot decipher between tornadic and nontornadic cells. Figures 4.2 and 4.3 show that maximum divergence and minimum divergence (convergence) appear to be good indicators between NOWARN and NTCs. With convergence and divergence both resulting as statistically significant between NOWARN and NTCs, it appears that the NOWARN cases are showing the updraft and downdraft

within the cell, resulting in tornado formation. If this is the case, forecasters may want to evaluate the divergence and convergence when faced with forecasting the tornadic potential isolated cells.

Almost all tornadoes in the dataset were F0 or F1. Of the 33 isolated tornadoes that did receive NWS warning, two were F2, 7 were F1, and the remaining 24 were F0. Of the 33 isolated tornadoes that did NOT receive NWS warning, 3 were F1 and the remaining 30 were F0. It has been noted by Brotzge and Donner (2013) that tornadoes associated with stronger convective systems are easier to warn for than weaker systems. This research further supports their findings, but also found significant differences among important kinematic tornado forecasting parameters. Although the majority of these tornadoes were weak, they still caused thousands of dollars of damage. One unwarned tornado caused \$100,000 worth of damage by itself. All unwarned tornadoes in this sample resulted in a damage total of \$385,000 compared to \$445,000 worth of damage caused by the tornadoes that were warned for in advance. Although most isolated tornadoes are classified as weak, they still cause damage to property and threaten public safety, and therefore cannot be pushed aside just because they are “weak”.

5.2 Future Work

If the goal of the NWS is to warn on every tornado 45 minutes prior to formation, more research needs to be conducted on isolated events as they prove to be the hardest to warn for in advance. As the climate is changing, tornadoes have become more frequent year round. Future work may want to exclude the limitation of months and analyze every month of the year. In addition to radar analysis, future work could make use of the

Tornado Detection Algorithm for a better understanding as to why some isolated events go unwarned. Shear parameters among isolated tornadoes also need to be evaluated more within a larger sample size; is there a threshold shear value for isolated tornadoes?

APPENDIX

```
%Examine characteristics of cells:  
%Reflectivity, composite reflectivity height, echo tops,  
%divergence @ 1km,2km, below 3km and 3-7km,  
  
%Runs for all time steps in a folder  
%Must change all path lengths for each case  
  
%individual identification change time and dates for all  
  
% SET THE REFLECTIVITY THRESHOLD  
z_thresh=35;  
  
%SET THE SIZE THRESHOLD (this sets the threshold for the images produced,  
%but also seems to work as a threshold for selecting cells in this version  
%of the routine  
size_thresh=20;  
  
%Setting paths for each variable  
%path = 'C:\Users\foxn\Documents\MATLAB\dualpol\7sep2012\z\02.00';  
path ='usr/local/wdss/vanburen/20130831_KBIS/merged/MergedReflectivity/02.00';  
path2 ='usr/local/wdss/vanburen/20130831_KBIS/merged/AzShearAtLowestAltitude/01.00';  
path3 ='usr/local/wdss/vanburen/20130831_KBIS/merged/AzShearMaxBelow3km/01.00';  
path4 =  
'usr/local/wdss/vanburen/20130831_KBIS/merged/DivergenceAtLowestAltitude/01.00';  
path5 ='usr/local/wdss/vanburen/20130831_KBIS/merged/EchoTop_30/01.00';  
path6 =  
'usr/local/wdss/vanburen/20130831_KBIS/merged/HeightAzShearMaxBelow3km/01.00';  
path7 ='usr/local/wdss/vanburen/20130831_KBIS/merged/RhoHVAAtLowestAltitude/01.00';  
path8 =  
'usr/local/wdss/vanburen/20130831_KBIS/merged/SpectrumWidthAtLowestAltitude/01.00';  
% Pulls file names of data files  
filenames = dir([path,'*.netcdf']);  
filenames2 = dir([path2,'*.netcdf']);  
filenames3 = dir([path3,'*.netcdf']);  
filenames4 = dir([path4,'*.netcdf']);  
filenames5 = dir([path5,'*.netcdf']);  
filenames6 = dir([path6,'*.netcdf']);
```

```

filenames7 = dir([path7,'/*.netcdf']);
filenames8 = dir([path8,'/*.netcdf']);
zstructure=struct;

for c = 1:length(filenames) %looping through all time steps in the folder
    disp(['Reading file Z ',filenames(c,1).name])
    filepathandname = [path,'/',filenames(c,1).name];
    ncid = netcdf.open(filepathandname,'NC_NOWRITE');

    rr=c;
    %time=regexp(filenames(i,1).name,'|-\d*|\.','match','once');
    SplitStr=regexp(filenames(c,1).name,'\\D','split');
    T=SplitStr(2);
    ti=cell2mat(T);
    time=str2num(ti);
    %T=vertcat(time);

    % Get the name of the first variable.
    [varname, xtype, varDimIDs, varAtts] = netcdf.inqVar(ncid,0);

    % Get variable ID of the first variable, given its name.
    varid = netcdf.inqVarID(ncid,varname);

    % Get the value of the first variable, given its ID.
    reflectivity=netcdf.getVar(ncid,varid)';
    [m n]=size(reflectivity);

    for ij=1:m
        for j=1:n
            if (reflectivity(ij,j)<=0)
                reflectivity(ij,j)=0;
            end
        end
    end

    %Setting size threshold for cells

    k=zeros(m,n);
    %Call function identifycells to qc data and find cells that reach z
    %threshold
    identifycells(z_thresh,reflectivity);

```

```

load ('labeled.txt');
if size(labeled) ~= size(reflectivity)
    labeled=zeros(m,n);
end
tempmax=max(labeled);
numberofcells=max(tempmax);

disp(['Reading file Az Shear At Lowest Altitude',filenames2(c,1).name])
filepathandname2 = [path2,'/',filenames2(c,1).name];
ncid2 = netcdf.open(filepathandname2,'NC_NOWRITE');

[varname2, xtype, varDimIDs, varAtts] = netcdf.inqVar(ncid2,0);
varid2 = netcdf.inqVarID(ncid2,varname2);
lowestazshear=netcdf.getVar(ncid2,varid2)';

for ij=1:m
    for j=1:n
        if (lowestazshear(ij,j)<=-10)
            lowestazshear(ij,j)=0;
        end
    end
end

disp(['Reading file Az Shear Below 3km',filenames3(c,1).name])
filepathandname3 = [path3,'/',filenames3(c,1).name];
ncid3 = netcdf.open(filepathandname3,'NC_NOWRITE');

[varname3, xtype, varDimIDs, varAtts] = netcdf.inqVar(ncid3,0);
varid3 = netcdf.inqVarID(ncid3,varname3);
azshearb3=netcdf.getVar(ncid3,varid3)';

for ij=1:m
    for j=1:n
        if (azshearb3(ij,j)<=-10)
            azshearb3(ij,j)=0;
        end
    end
end

disp(['Reading file Divergence',filenames4(c,1).name])
filepathandname4 = [path4,'/',filenames4(c,1).name];
ncid4 = netcdf.open(filepathandname4,'NC_NOWRITE');

```

```

[varname4, xtype, varDimIDs, varAtts] = netcdf.inqVar(ncid4,0);
varid4 = netcdf.inqVarID(ncid4,varname4);
divergence=netcdf.getVar(ncid4,varid4)';

for ij=1:m
    for j=1:n
        if (divergence(ij,j)<=-10)
            divergence(ij,j)=0;
        end
    end
end

disp(['Reading file Echo Top',filenames5(c,1).name])
filepathandname5 = [path5,'/',filenames5(c,1).name];
ncid5 = netcdf.open(filepathandname5,'NC_NOWRITE');

[varname5, xtype, varDimIDs, varAtts] = netcdf.inqVar(ncid5,0);
varid5 = netcdf.inqVarID(ncid5,varname5);
echotop=netcdf.getVar(ncid5,varid5)';

for ij=1:m
    for j=1:n
        if (echotop(ij,j)<=-10)
            echotop(ij,j)=0;
        end
    end
end

disp(['Reading file Height Az Shear',filenames6(c,1).name])
filepathandname6 = [path6,'/',filenames6(c,1).name];
ncid6 = netcdf.open(filepathandname6,'NC_NOWRITE');

[varname6, xtype, varDimIDs, varAtts] = netcdf.inqVar(ncid6,0);
varid6 = netcdf.inqVarID(ncid6,varname6);
azshearht=netcdf.getVar(ncid6,varid6)';

for ij=1:m
    for j=1:n
        if (azshearht(ij,j)<=-10)
            azshearht(ij,j)=0;
        end
    end
end

```

```

    end
end

disp(['Reading file Rho HV',filenames7(c,1).name])
filepathandname7 = [path7,'/',filenames7(c,1).name];
ncid7 = netcdf.open(filepathandname7,'NC_NOWRITE');

[varname7, xtype, varDimIDs, varAtts] = netcdf.inqVar(ncid7,0);
varid7 = netcdf.inqVarID(ncid7,varname7);
rhohv=netcdf.getVar(ncid7,varid7);

for ij=1:m
    for j=1:n
        if (rhohv(ij,j)<=-10)
            rhohv(ij,j)=0;
        end
    end
end

disp(['Reading file SW at Lowest',filenames8(c,1).name])
filepathandname8 = [path8,'/',filenames8(c,1).name];
ncid8 = netcdf.open(filepathandname8,'NC_NOWRITE');

[varname8, xtype, varDimIDs, varAtts] = netcdf.inqVar(ncid8,0);
varid8 = netcdf.inqVarID(ncid8,varname8);
lowestSW=netcdf.getVar(ncid8,varid8);

for ij=1:m
    for j=1:n
        if (lowestSW(ij,j)<=-10)
            lowestSW(ij,j)=0;
        end
    end
end

zarray=zeros(numberofcells,26);

for e=1:numberofcells
    for i=1:m
        for j=1:n
            if labeled(i,j)==e
                z(i,j)= reflectivity(i,j);
            end
        end
    end
end

```

```

az(i,j)= lowestazshear(i,j);
az03(i,j)= azshearb3(i,j);
div(i,j)= divergence(i,j);
et(i,j)= echotop(i,j);
azht(i,j)= azshearht(i,j);
rhv(i,j)= rhohv(i,j);
sw(i,j)= lowestSW(i,j);

else
    z(i,j)=0;
    az(i,j)=0;
    az03(i,j)=0;
    div(i,j)=0;
    et(i,j)=0;
    azht(i,j)=0;
    rhv(i,j)=0;
    sw(i,j)=0;
end
end
end

for i=1:m
    for j=1:n
        if z(i,j)>0
            numpixelstemp(i,j)=1;
        else
            numpixelstemp(i,j)=0;
        end
    end
end
numpixelstemp2=sum(numpixelstemp);
numpixelsincell=sum(numpixelstemp2);

%time=regexp(filenames(i,1).name,'\\d+\\.','match','once');

if numpixelsincell>size_thresh

    %find max and min axes for elliplabeled(i,j)==ese and area
    for i=1:m
        for j=1:n
            if (z(i,j)>0)
                zid(i,j)=1;
            else

```

```

        zid(i,j)=0;
    end
end
end

for degree=1:180
    rotimage=rotate_image( degree, zid, [1,m;1,n]);
    maxaxis(degree)=max(sum(rotimage));
end

[x y]=find(numpixelstemp==1);
xmed=median(x);
ymed=median(y);

axis1=max(maxaxis);
axis2=min(maxaxis);
eliparea=pi()*(axis1/2)*(axis2/2);
orient=find(max(maxaxis)==maxaxis);

testimages=reshape(z,m*n,1);
azimages=reshape(az,m*n,1);
az03images=reshape(az03,m*n,1);
divimages=reshape(div,m*n,1);
etimages=reshape(et,m*n,1);
azhtimages=reshape(azht,m*n,1);
rhvimages=reshape(rhv,m*n,1);
swimages=reshape(sw,m*n,1);

for np=1:numpixelsincell
    statarray(np)=0;
    statarrayaz(np)=0;
    statarrayaz03(np)=0;
    statarraydiv(np)=0;
    statarrayet(np)=0;
    statarrayazht(np)=0;
    statarrayrv(np)=0;
    statarraysw(np)=0;

end

a=1;
for b=1:(m*n)

```

```

if testimages(b)>0
    statarray(a)=statarray(a)+testimages(b);
    a=a+1;
end
end

p=1;
for i=1:(m*n)
    if azimages(i)~=0
        statarrayaz(p)=statarrayaz(p)+azimages(i);
        p=p+1;
    end
end

p=1;
for i=1:(m*n)
    if az03images(i)~=0
        statarrayaz03(p)=statarrayaz03(p)+az03images(i);
        p=p+1;
    end
end

p=1;
for i=1:(m*n)
    if divimages(i)~=0
        statarraydiv(p)=statarraydiv(p)+divimages(i);
        p=p+1;
    end
end

p=1;
for i=1:(m*n)
    if etimages(i)~=0
        statarrayet(p)=statarrayet(p)+etimages(i);
        p=p+1;
    end
end

p=1;
for i=1:(m*n)
    if azhtimages(i)~=0
        statarrayazht(p)=statarrayazht(p)+azhtimages(i);
    end

```

```

    p=p+1;
end
end

p=1;
for i=1:(m*n)
    if rhvimages(i)~=0
        statarrayrv(p)=statarrayrv(p)+rhvimages(i);
        p=p+1;
    end
end

p=1;
for i=1:(m*n)
    if swimages(i)~=0
        statarraysw(p)=statarraysw(p)+swimages(i);
        p=p+1;
    end
end

meanintensityincell=mean(statarray);
maxintensityincell=max(statarray);
minintensityincell=min(statarray);
standdevincell=std(statarray);
ratio=axis1/axis2;

maxazshear=max(statarrayaz);
meanazshear=mean(statarrayaz);
minazshear=min(statarrayaz);
maxazshearbelow3=max(statarrayaz03);
minazshearbelow3=min(statarrayaz03);
meanazshearbelow3=mean(statarrayaz03);
maxdivergence=max(statarraydiv);
mindivergence=min(statarraydiv);
meandivergence=mean(statarraydiv);
maxechotop=max(statarrayet);
minrhohv=min(statarrayrv);
meanrhohv=mean(statarrayrv);
maxsw=max(statarraysw);
meansw=mean(statarraysw);

zarrayheader=char('Time','CellID','CellSize','MaxdBZ','MeandBZ','MindBZ','StdBZ','majaxi

```

```

s','minaxis','ratio','centroid_x','centroid_y');
%
zarray(1,1)=time;
zarray(e,2)=e;
zarray(e,3)=xmed;
zarray(e,4)=ymed;
zarray(e,5)=numpixelsincell;
zarray(e,6)=maxintensityincell;
zarray(e,7)=meanintensityincell;
zarray(e,8)=minintensityincell;
zarray(e,9)=standdevincell;
zarray(e,10)=maxazshear;
zarray(e,11)=minazshear;
zarray(e,12)=meanazshear;
zarray(e,13)=maxazshearbelow3;
zarray(e,14)=minazshearbelow3;
zarray(e,15)=meanazshearbelow3;
zarray(e,16)=maxdivergence;
zarray(e,17)=mindivergence;
zarray(e,18)=meandivergence;
zarray(e,19)=maxechotop;
zarray(e,20)=minrhohv;
zarray(e,21)=meanrhohv;
zarray(e,22)=maxsw;
zarray(e,23)=meansw;
zarray(e,24)=axis1;
zarray(e,25)=axis2;
zarray(e,26)=ratio;

```

```

f=find(zarray(:,2)>0);
f=[1 f'];
zar=zarray(f,:);

zstructure(rr).cells=zar;
%zstructure(rr).cellimage=labeled;

```

```

for s=1:length(f)
    t=labeled==f(s);
    k=k+t;
end

```

```
statarray=0;

end
end

figure
subplot(211)
imagesc(k.*lowestazshear);
colormap(hsv)
caxis([-0.05 0.05]);
colorbar;
subplot(212)
imagesc(k.*azshearb3);
colormap(hsv)
caxis([-0.05 0.05]);
colorbar;

end
```

REFERENCES

- Brotzge, J. and S. Erickson, 2009: NWS Tornado Warnings with Zero or Negative Lead Times. *Weather and Forecasting*, **24**, 140-154.
- Brotzge, J., and S. Erickson, 2010: Tornadoes without NWS Warning. *Weather and Forecasting*, **25**, 159-172.
- Brotzge, J., and W. Donner, 2013: The Tornado Warning Process: A Review of Current Research, Challenges, and Opportunities. *American Meteorological Society*, 1715-1726.
- Brotzge, J. A., S. E. Nelson, R. L. Thompson and B. T. Smith, 2013: Tornado Probability of Detection and Lead Time as a Function of Convective Mode and Environmental Parameters. *American Meteorological Society*, **28**, 1261-1276.
- Grams, J. S., R. L. Thompson, D. V. Snively, J. A. Prentice, G. M. Hodges and L. J. Reames, 2011: A Climatology and Comparison of Parameters for Significant Tornado Events in the United States. *Weather and Forecasting*, **27**, 106-123.
- Klemp, J., and R. Rotunno, 1983: A Study of the Tornadic Region within a Supercell Thunderstorm. *Journal of the Atmospheric Sciences*, **40**, 359-377.
- Kumjian, M. R., 2013: Principles and Applications of Dual-Polarization Weather Radar. Part I: Description of the Polarimetric Radar Variables. *J. Operational Meteor.*, **1** (19), 226-242.
- Lack, S. A., and N. I. Fox, 2012: Development of an automated approach for identifying convective storm type using reflectivity-derived and near-storm environment data. *Atmospheric Research*, **116**, 67–81.

Lakshmanan, V., T. Smith, K. Hondl, G. J. Stumpf, and A. Witt, 2006: A Real-Time, Three-Dimensional, Rapidly Updating, Heterogeneous Radar Merger Technique for Reflectivity, Velocity, and Derived Products. *Weather and Forecasting*, **21**, 802–823.

Lakshmanan, V., T. Smith, G. Stumpf, and K. Hondl, 2007: The Warning Decision Support System—Integrated Information. *Weather and Forecasting*, **22**, 596-612.

NOAA, 2017: History of Tornado Forecasting. [Available online at https://celebrating200years.noaa.gov/magazine/tornado_forecasting/#intro]

Serafin, R. J., and J. W. Wilson, 2000: Operational Weather Radar in the United States: Progress and Opportunity. *Bulletin of the American Meteorological Society*, **81** (3), 501-518.

Smith, B. T., R. L. Thompson, J. S. Grams, C. Broyles, and H. E. Brooks, 2012: Convective Modes for Significant Severe Thunderstorms in the Contiguous United States. Part I: Storm Classification and Climatology. *Weather and Forecasting*, **27**, 1114-1135.

Stensrud, D. J., M. Xue, L. J. Wicker, K. E. Kelleher, M. P. Foster, J. T. Schaefer, R. S. Schneider, S. G. Benjamin, S. S. Weygandt, J. T. Ferree, and J. P. Tuell, 2009: Convective-Scale Warn-On-Forecast System: A Vision for 2020. *American Meteorological Society*, 1487-1499.

Thompson, R. L., B. T. Smith, J. S. Grams, A. R. Dean, and C. Broyles, 2012: Convective Modes for Significant Severe Thunderstorms in the Contiguous United States. Part II: Supercell and QLCS Tornado Environments. *Weather and Forecasting*, **27**, 1136-1154.

Whiton, R. C., P. L. Smith, S. G. Bigler, K. E. Wilk, and A. C. Harbuck, 1998: History of Operational Use of Weather Radar by U.S. Weather Services. Part I: The Pre-NEXRAD Era. *Bulletin of the American Meteorological Society*, 219-243.